Oncogene (2013) **32,** 5522–5530

www.nature.com/onc

OPEN

ORIGINAL ARTICLE

Telomere dysfunction and activation of alternative lengthening of telomeres in B-lymphocytes infected by Epstein–Barr virus

SA Kamranvar[1,2], X Chen[1,2] and MG Masucci[1]

Malignant cells achieve replicative immortality by two alternative mechanisms, a common one dependent on *de novo* synthesis of telomeric DNA by telomerase, and a rare one based on telomere recombination known as alternative lengthening of telomeres (ALT). Epstein–Barr virus (EBV) transforms human B-lymphocytes into lymphoblastoid cell lines with unlimited growth potential *in vitro* and *in vivo*. Here we show that newly EBV-infected cells exhibit multiple signs of telomere dysfunction, including the occurrence of extra-chromosomal telomeres, telomere fusion and telomere length heterogeneity, and undergo progressive increase in telomere length without a parallel increase in telomerase activity. This phenotype is accompanied by the accumulation of telomere-associated promyelocytic leukemia nuclear bodies and telomeric-sister chromatid exchange, suggesting that EBV infection promotes the activation of ALT. Newly infected cells also display a significant reduction of telomere-associated TRF2 and express low levels of TRF1, TRF2, POT1 and ATRX, pointing to telomere de-protection as an important correlate of ALT activation. Collectively, these findings highlight the involvement of recombination-dependent mechanisms for maintenance of telomere homeostasis in EBV-induced B-cell immortalization.

Oncogene (2013) **32,** 5522–5530; doi:10.1038/onc.2013.189; published online 27 May 2013

Keywords: EBV; telomere; telomerase; ALT; shelterin; TRF2

INTRODUCTION

Telomeres are nucleoprotein structures that protect the ends of linear chromosomes.[1] Human telomeric DNA consists of a 3–12 kb long tandem array of the hexanucleotide 5′-TTAGGG-3′ [2] that ends in a 50–200 nucleotides long single-strand 3′ overhang whose invasion into the duplex region results in the formation of a telomeric loop.[3,4] The telomeres are coated by a protein complex, known as shelterin, composed of the TRF1, TRF2, POT1, TIN2, TPP1 and RAP1 subunits.[5] TRF1 and TRF2 bind to double-stranded telomeric DNA, whereas POT1 associates with the single-strand 3′ overhang.[6] The remaining subunits connect the double-stranded DNA with the single-strand overhang. Thus, TRF1 and TRF2 interact with TIN2, TPP1 binds to POT1 and TIN2, and TRF2 forms a complex with RAP1.[7,8] The shelterin complex prevents the recognition of telomeres as damaged DNA and regulates telomere length maintenance.[5] TRF1 is the main negative regulator of telomere length,[9] whereas TRF2 and POT1 suppress the DNA damage response through inhibition of the ATM and ATR signaling pathways.[10,11] Loss of TRF2 activates the ATM kinase, leading to p53 upregulation and p21-mediated G1/S arrest.[12] Altered expression of the shelterin subunits is accompanied by the formation of telomere dysfunction-induced foci (TIFs) that contain a variety of DNA damage response and repair proteins, including phosphorylated histone H2AX, the Mre11, Rad50 and Nbs1 complex, phosphorylated ATM and 53BP1.[13–16]

The telomeres are shortened at each cell division because of incomplete replication of the chromosome termini. When the length falls below a critical threshold, p53 is activated and induces p16- and retinoblastoma protein-dependent replicative senescence.[17,18] Tumor cells escape this proliferation barrier by activating functions that preserve the length of telomeres. In most cancers, this is achieved by upregulating the activity of telomerase,[18] whereas a telomerase-independent mechanism, referred to as alternative lengthening of telomeres (ALT), operates in 10–15% of the tumors.[19–22] In ALT-positive cells, telomere elongation is mainly accomplished by homologous recombination (HR) of telomeric sequences. This process is repressed by TRF2, POT1, RAP1 and the Ku70/80 heterodimer in telomerase-positive cells.[23–26] Hallmarks of ALT activation include the accumulation of extra-chromosomal telomere sequences, frequently t-circles and C-circles, heterogeneous length of telomeres, presence of promyelocytic leukemia (PML) nuclear bodies (PNB) containing telomeric DNA (APBs), and elevated rates of telomeric-sister chromatid exchange telomeric sister chromatid exchange (T-SCE).[21,22] Furthermore, mutations in the ATRX/DAXX chromatin-remodeling complex and loss of the histone H3.3 variant are frequently observed,[27] suggesting that defects in the organization of telomeric chromatin could have an important role in the activation of ALT.

Epstein–Barr virus (EBV) is a human lymphotropic herpesvirus implicated in the pathogenesis of a broad spectrum of lymphoid and epithelial cell malignancies including post-transplant lymphomas, endemic Burkitt's lymphoma (BL), nasopharyngeal carcinoma, and a subset of Hodgkin's disease lymphomas and gastric carcinomas.[28] EBV establishes non-productive infections in B-lymphocytes characterized by the expression of a restricted repertoire of latency-associated viral genes that encode for six EBV nuclear antigens (EBNA1, − 2, − 3A, − 3B, − 3C and − LP), three latent membrane proteins (LMP1, − 2A, − 2B), two non-translated RNAs (EBER1 and EBER2) and several microRNAs.[29,30] The latency products promote B-cell proliferation, which allows access to the memory B-cell compartment where the virus persists as a life-long

Department of Cell and Molecular Biology, Karolinska Institute, Stockholm, Sweden. Correspondence: Professor MG Masucci, Department of Cell and Molecular Biology, Karolinska Institutet, Box 285, Stockholm 171 77, Sweden. E-mail maria.masucci@ki.se
[2]These authors contributed equally to this work.
Received 13 February 2013; revised 28 March 2013; accepted 9 April 2013; published online 27 May 2013

asymptomatic infection that is under tight immunological control. Loss of specific immunity promotes the development of EBV-carrying immunoblastic lymphomas in immunosuppressed patients,[31] which is paralleled by the spontaneous outgrowth of EBV-transformed lymphoblastoid cell lines (LCLs) on explant of blood lymphocytes from EBV-seropositive healthy donors under conditions that prevent T-cell activation.[32]

Several studies have documented the capacity of EBV latency proteins to regulate the activity of telomerase. For example, LMP1 expression was shown to enhanced the activity of telomerase in B-cell lines, primary epithelial cell cultures and nasopharyngeal carcinoma cell lines,[33–35] whereas the expression of LMP2A is accompanied by reduction of hTERT mRNA and silencing of the hTERT promoter in tumor cell lines.[36] However, the importance of telomerase for EBV-induced immortalization is questioned by the finding that newly established LCLs often exhibit very low telomerase activity, whereas strong activation is only observed after >150 population doublings *in vitro*.[37] Furthermore, the average length of telomeres did not decrease significantly during the first months in culture,[38,39] suggesting the involvement of telomerase-independent mechanisms for maintenance of telomere homeostasis.

In this study, we sought to assess whether ALT may be active in newly EBV-infected B-lymphocytes. We report that within the first month of culture rapidly proliferating EBV-infected cells exhibit multiple signs of telomere dysfunction and ALT activation, including the accumulation of extra-chromosomal telomeres and APBs, increased telomere length, telomere length heterogeneity and T-SCE. Several subunits of the shelterin and ATRX/DAXX complexes are poorly expressed in newly established LCLs suggesting that telomere de-protection may contribute to the activation of recombination-dependent mechanisms for maintenance of telomere homeostasis during EBV-induced B-cell immortalization.

RESULTS

Telomere abnormalities in newly EBV-infected B cells

In order to assess whether EBV infection promotes telomere dysfunction we first monitored the occurrence of telomere abnormalities by quantitative fluorescence *in situ* hybridization (Q-FISH) staining of metaphase chromosomes from EBV-infected and mitogen-induced B- or T-cell blasts. Monitoring of cell division by analysis of CFSE fluorescence (Figure 1A) confirmed the induction of comparable levels of cell proliferation, with most of the cells having undergone six or more cell divisions by day 10 (Figure 1B). Expression of the EBV nuclear antigens EBNA2 and EBNA1 was demonstrates by immunofluorescence staining in a large majority of the infected cells by day 7 (EBNA2 $88 \pm 5\%$, EBNA1 $72 \pm 12\%$). Comparable levels of cell proliferation, assessed by counting the number of live cells detected by Trypan blue dye exclusion, were maintained for up to 3 weeks, after which increasing cell death was observed in the mitogen-stimulated cultures (data not shown). A high prevalence of chromosomes with abnormal telomeres (Figure 1C), usually loss or duplication of telomere signals and telomere fusion, was detected already during the first week after EBV infection (Figure 1D). Between 50–60% of the metaphases of EBV-infected cells contained one or more chromosomes with abnormal telomeres on day 7. The proportion of atypical metaphases stabilized to approximately 30% during the following weeks. In contrast, telomere abnormalities were detected in $<10\%$ of the metaphases from mitogen-induced blasts throughout the observation period. Extra-chromosomal telomere signals (Figure 1E) were frequently detected in metaphase spreads of EBV-infected cells, indicating double-strand breaks of telomeric DNA (Figure 1F). The occurrence of abnormal telomeres (Figure 2a) and extra-chromosomal telomeres (Figure 2b) was greatly reduced in established LCLs kept in culture for extended periods of time.

EBV infection induces telomere elongation in the absence of telomerase activity

In order to further investigate the effect of EBV infection on the functionality of telomeres, changes in telomere length were monitored over time by measuring the intensity of the telomere signals in micrographs of FISH-stained metaphase plates. This Q-FISH methodology affords a distinct advantage compared with analysis of telomere length by Southern blot because it provides information on the size of individual telomeres in mitotic cells and avoids possible artifacts due to the presence of variable amounts of non-proliferating or dead cells during the early phases of the cultures. A first analysis performed on EBV- and mitogen-induced blasts kept in culture for approximately 3 weeks revealed stronger signals in the virus-infected cells (Figure 3a). To examine the validity of this observation, the intensity of telomere signals was monitored weekly during the first 4 weeks of culture. As shown in Figure 3b, a modest but significant increase in the average intensity of telomere signals was detected in the chromosomes of 25 randomly selected metaphases from EBV-infected cells starting from the second week of culture. In contrast, the average intensity of telomeres from mitogen-induced blasts did not change significantly during 3 weeks, after which the analysis was discontinued because of a significant drop in cell viability. Notably, the intensity of the telomere signals was highly heterogeneous in EBV-infected cells, with a strongest:weakest signal ratio exceeding 50-fold, whereas the ratio was <10-fold in the mitogen blasts (Figure 3c).

The activation of telomerase is the most common mechanism for maintenance of telomere length in mammalian cells.[18] In order to monitor changes in the activity of telomerase over time, telomeric repeat amplification protocol (TRAP) assays were performed with cell lysates from EBV-infected and mitogen-stimulated cells. As illustrated by the representative assay shown in Figure 3d, the activity of telomerase assessed by the intensity of the amplified products was very low in both EBV- and mitogen-induced blasts throughout the monitoring period. The mean total product generated units recorded in three independent experiments where the two types of blasts were tested in parallel in shown Figures 3e. A two- to threefold increase over baseline levels was observed on day 3 in both conditions, followed by a rapid decline. Of note, comparably low levels of activity were recorded on day 14 when the telomere signals were significantly stronger in EBV-infected cells. Thus, EBV infection promotes the increase in telomere length in the absence of a parallel increase in telomerase activity.

It was previously reported that the activation of telomerase is a late event in EBV-induced B-cell immortalization.[39] We compare therefore telomerase activity measured by TRAP assay (Figure 4a), and telomere length measured by Q-FISH, in a panel of six newly established LCLs cultured for approximately 1 month, and six old LCLs that were kept in culture for >5 years. As shown in Figure 4b, in four of the six newly established LCLs the activity of telomerase was within the limits of the background detected in the telomerase-negative U2OS cell line, and a minor increase was observed in two LCLs, whereas substantially higher levels of activity were regularly detected in the old LCLs. In addition, the old LCLs exhibited short telomeres with homogeneous length distribution, whereas the telomeres were longer and highly heterogeneous in the newly established LCLs (Figure 4b). The observation of shorter telomeres in cells expressing higher levels of telomerase is consistent with earlier reports showing that enforced expression of telomerase in telomerase-negative tumor cell lines is associated with the inhibition of recombination-based telomere elongation and progressive loss of long telomeres.[40]

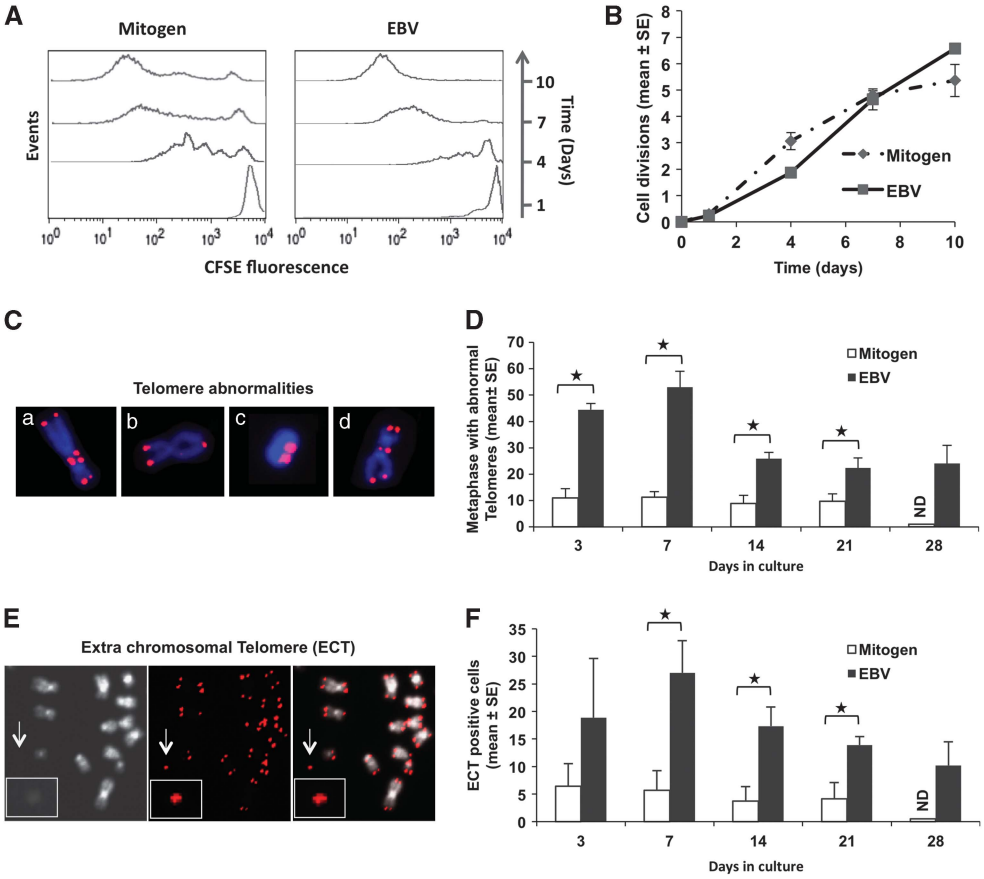

Figure 1. EBV infection induces telomere dysfunction. (**A**) Representative experiment illustrating the comparable levels of cell proliferation recorded in mitogen-stimulated and EBV-infected cultures assessed by carboxyfluorescein diacetate succinimidyl ester (CFSE) dye incorporation. (**B**) Average number of cell division assessed by CFSE assays during the first 10 days of culture. Mean ± s.e. of three experiments. (**C**) Representative micrographs illustrating the telomere abnormalities scored in metaphase plates of EBV-infected and mitogen-induced blasts. (**A**) heterogeneous telomere signals and chromosome juxtaposition by telomere fusion, (**B**) telomere fusion, (**C**) chromosome circle with telomere fusion, (**D**) juxtaposition of chromosomes with telomere fusion. Telomeres were stained by Q-FISH (red) and chromosomes were stained by 4,6-diamidino-2-phenylindole (DAPI; blue). (**D**) Mean ± s.e. metaphases with telomere abnormalities in three independent experiments where EBV-infected and mitogen-induced blasts were tested in parallel. At least 25 metaphase plates were tested for each time point and condition. (**E**) Representative Q-FISH illustrating the occurrence of extra-chromosomal telomeres (ECT, arrows) in EBV-infected cells. The chromosomes were stained with DAPI (gray). (**F**) Quantification of the number of cells with ECT in EBV-infected and mitogen-stimulated cultures. Mean ± s.e. of three experiments. $^{*}P < 0.05$.

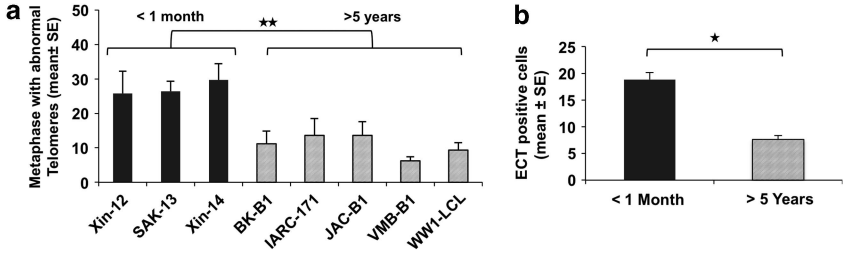

Figure 2. Signs of telomere dysfunction decrease in old LCLs. (**a**) Quantification of metaphases with telomere abnormalities in newly established and old LCLs. Mean ± s.e. of three experiments. $^{**}P < 0.01$. (**b**) Mean ± s.e. of ECT-positive metaphases in newly established ($n = 3$) and old LCLs ($n = 6$). Twenty-five metaphases were tested for each cell line in two independent experiments. $^{*}P < 0.05$.

EBV infection activates HR-based telomere elongation

The accumulation of extra-chromosomal telomeres and increased telomere length in the absence of telomerase activity are indicative for the activation of a recombination-based mechanisms for maintenance of telomere homeostasis known as ALT.[41] A recognized marker of ALT is the accumulation of PML nuclear bodies (PNBs) containing telomeric DNA known as ALT-associated PNBs (APBs).[22] In addition to PML, APBs contain a variety of proteins involved in the DNA damage response, and polymerases that use sister chromatids or extra-chromosomal telomeric sequences as templates for telomere extension.[42] The occurrence of APBs was monitored by immunofluorescence-FISH staining for telomeres and PML in interphase nuclei of EBV-infected cells and mitogen-induced B-blast. APBs, identified by the colocalization of PML and telomere fluorescence in a single focal plane (Figure 5a), were virtually absent in freshly isolated cells

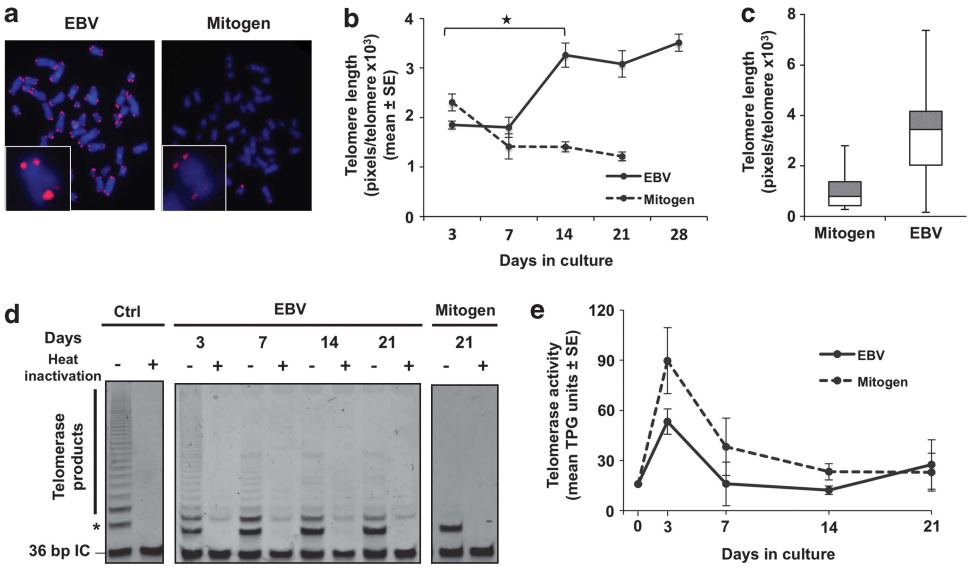

Figure 3. EBV infection promotes lengthening of telomeres in the absence of telomerase activity. (**a**) Representative micrographs of Q-FISH-stained metaphase plates illustrating the heterogeneity of telomere signals in EBV-infected cells compared with mitogen-induced blasts. The chromosomes were stained by 4,6-diamidino-2-phenylindole (DAPI). (**b**) Quantification of the average intensity of telomere signals in EBV-infected and mitogen-induced blasts. Mean ± s.e. of the number of pixels/telomere in three independent experiments. Twenty-five metaphase plates were analyzed per each time point and condition. (**c**) Box plots of the intensity of telomere signals in 25 randomly selected metaphase plates from EBV-infected and mitogen-induced blasts on day 21 of culture. (**d**) Representative SYBR gold-stained polyacrylamide gels of TRAP assay performed with cell extract from EBV-infected and mitogen-induced blasts harvested at different times after infection. The control lanes illustrate the size of the telomere template and 6-bp extension ladder obtained with the reference telomerase-positive cell extract provided by the kit. The 36-bp bands at the bottom represent the internal PCR control. The asterisk indicates a nonspecific band detected in most of the assays. (**e**) Mean ± s.e. of total product generated (TPG) units in three independent experiments.

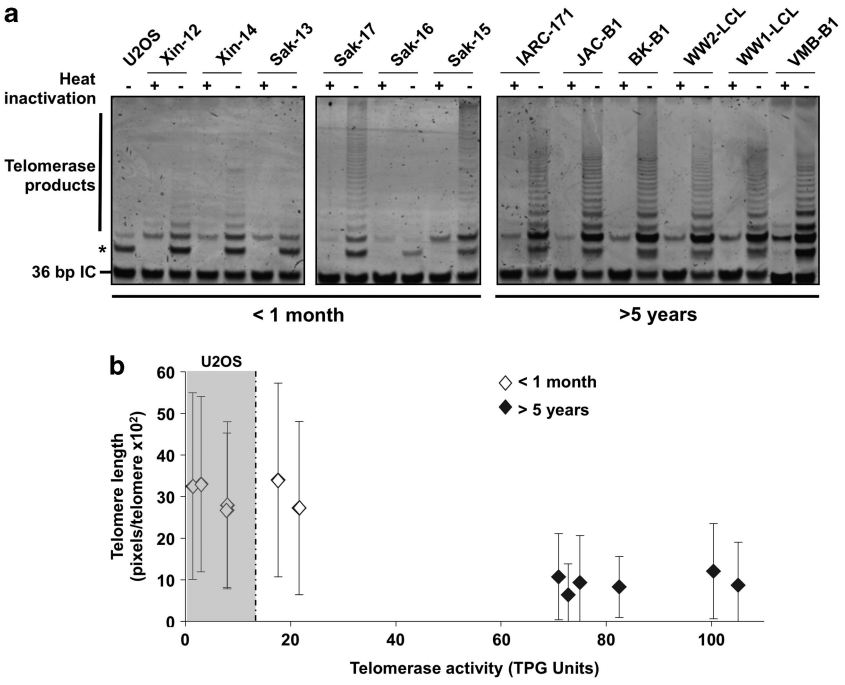

Figure 4. Inverse correlation between telomerase activity and telomere length distribution in newly established and old LCLs. (**a**) Representative SYBR gold-stained polyacrylamide gels of TRAP assay performed with untreated and heat-inactivated protein extract from newly established and old LCLs. Cell extracts from the telomerase-negative U2OS cell lines were used as control. (**b**) Plot illustrating the inverse correlation between telomerase activity, expressed in total product generated (TPG) units, and telomere length, measured as number of pixel per telomere, in newly established and old LCLs. The TPG units are the mean of three independent experiments and telomere length was obtained by measuring individual telomeres in 25 metaphase plates. The shaded area indicates the background levels of telomerase activity detected in lysates of U2OS cells (mean + 2 s.d.).

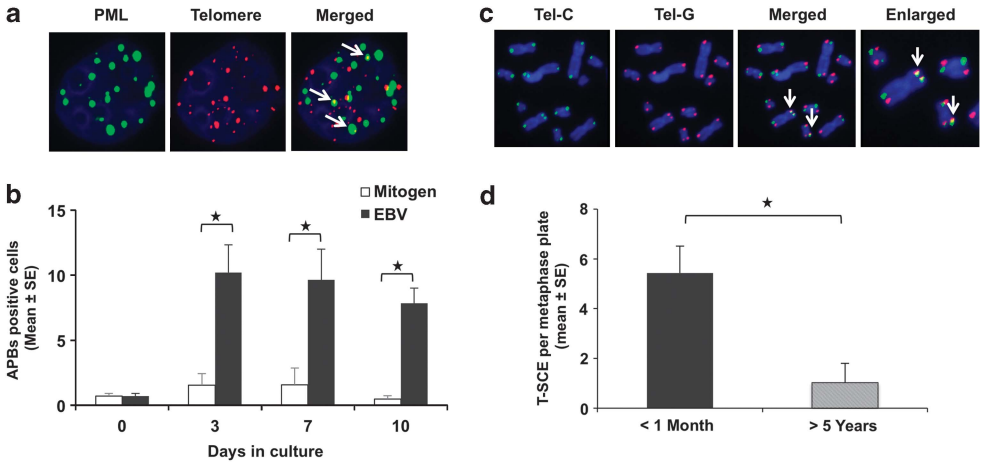

Figure 5. Telomere-associated DNA damage and HR in freshly EBV-infected cells. (**a**) Representative immunofluorescence-FISH (IF-FISH) micrographs illustrating the presence of APBs in EBV-infected primary B cells. (**b**) Mean ± s.e. of cell containing at least two or more APBs in EBV-infected and mitogen-stimulated blasts. At least 25 nuclei per each condition and time point were scored in three independent experiments. $^*P < 0.05$. (**c**) Representative micrographs illustrating the occurrence of telomere-sister chromatid exchange in EBV-infected cells. Chromosome orientation (CO)-FISH was performed with the telomere strand-specific probes TelC (leading strand template, red) and TelG (lagging strand template, green). Telomere sister chromatid exchange is visualized by colocalization of red and green signals on the same telomere (arrows). (**d**) Mean ± s.e. of telomere-sister chromatid exchange-positive chromosomes. Approximately 1000 metaphase chromosomes were score in six newly established and six old LCLs in two independent experiments. $^*P < 0.05$.

(Figure 5b). A significant increase was regularly detected already after 3 days in the EBV-infected cells and the proportion of APBs remained high during subsequent culture, whereas only a small and transient increase was observed in mitogen-induced blasts (Figure 5b).

EBV-induced B-cell proliferation is associated with a transient induction of high levels of DNA damage,[43] which was confirmed in our analysis by a significant increase in the number and size of PNBs (data not shown). Thus, we cannot formally exclude that the increase in APBs in interphase nuclei may be partially explained by chance colocalization of PNBs with telomere signals. In order to address this possible artifact and directly probe for the activation of ALT, we monitored the occurrence of T-SCE by chromosome orientation-FISH. In this assay, the recombination of telomeres derived from sister chromatids is visualized in metaphase chromosomes hybridized with C-rich (leading strand template, Figure 5c, green) and G-rich (lagging strand template, Figure 5c, red) probes by the colocalization of green and red fluorescence in a single telomere signal. Analysis of the prevalence of T-SCE in a panel of LCLs cultured for approximately 1 month or >5 years revealed significantly higher levels of T-SCE in the young LCLs, confirming that HR of telomeric sequences occurs in these cells. The activation of telomerase in old LCLs was accompanied by reduction of T-SCE to nearly undetectable levels (Figure 5d). Collectively, these findings suggest that during the early phases of B-cell immortalization EBV exploits recombination-based mechanisms to assure the maintenance of telomere homeostasis in rapidly proliferating cells with low or absent telomerase activity.

EBV infection promotes telomere de-protection

Telomere de-protection is a common cause of DNA damage at telomeres.[44] In order to assess whether uncapping might explain the telomere dysfunction phenotype induced by EBV infection, the functionality of the shelterin complex was investigated by monitoring the colocalization of telomeres with the DNA-binding subunit TRF2 in immunofluorescence-FISH assays. As illustrated by the representative micrographs shown in Figure 6a, telomeres lacking colocalized TRF2 signals were frequent in the interphase nuclei of EBV-infected cells cultured for 2 weeks. Quantitative analysis of the extent of colocalization, measured as the ratio between the intensities of the telomere and colocalized TRF2 signals revealed a significantly decreased TRF2:telomere signal ratio in the virus-infected cells compared with mitogen-induced blasts (Figure 6b). To assess whether this may correlate with defects in the expression of TRF2 or other proteins involved in the maintenance of telomere structure, the expression of the shelterin subunits TRF1, TRF2 and POT1, and the ATRX subunit of the ATRX/DAXX chromatin remodeler was compared in western blots. As illustrated in Figure 6c where two pairs of EBV-infected and mitogen-induced blasts were tested in parallel, and summarized by the densitometry analysis of five independent experiments shown in Figure 6d, the cells expressed comparable levels of all proteins. Thus, the telomere de-protection observed in EBV-infected cells is not due to selective loss of the shelterin or ATRX/DAXX complexes. To explore this phenomenon further, the expression of shelterin and ATRX/DAXX subunits was investigated by western blot in a panel of six newly established and six old LCLs. As illustrated by the representative blot shown in Figures 7a and b, and summarized by the densitometry of three independent experiments shown in Figures 7c and d, TRF1, TRF2, POT1, TIN2 and ATRX were expressed at significantly lower levels in the newly established LCLs.

DISCUSSION

The evasion of proliferative senescence is a key event in viral oncogenesis. Many tumor viruses, most notably KSHV, HPV, HCV and HTLV1, achieve this goal by regulating the activity of telomerase, which maintains the length of telomeres and ensures proliferative immortality (reviewed in Bellon and Nicot[45]). Here we have provided evidence for the capacity of EBV-infected cells to adopt an alternative strategy for maintenance of telomere homeostasis based on the activation of HR. We have shown that newly infected B-lymphocytes exhibit multiple signs of telomere dysfunction and activation of recombination-based ALT. Specifically, within the first month after infection, rapidly proliferating B-lymphocytes showed highly heterogeneous telomeres and progressive increase in the average telomere length in the absence of a parallel increase in telomerase activity. Other pathognomonic signs of ALT activation include: (i) the appearance of extra-chromosomal telomeric DNA, which reflects

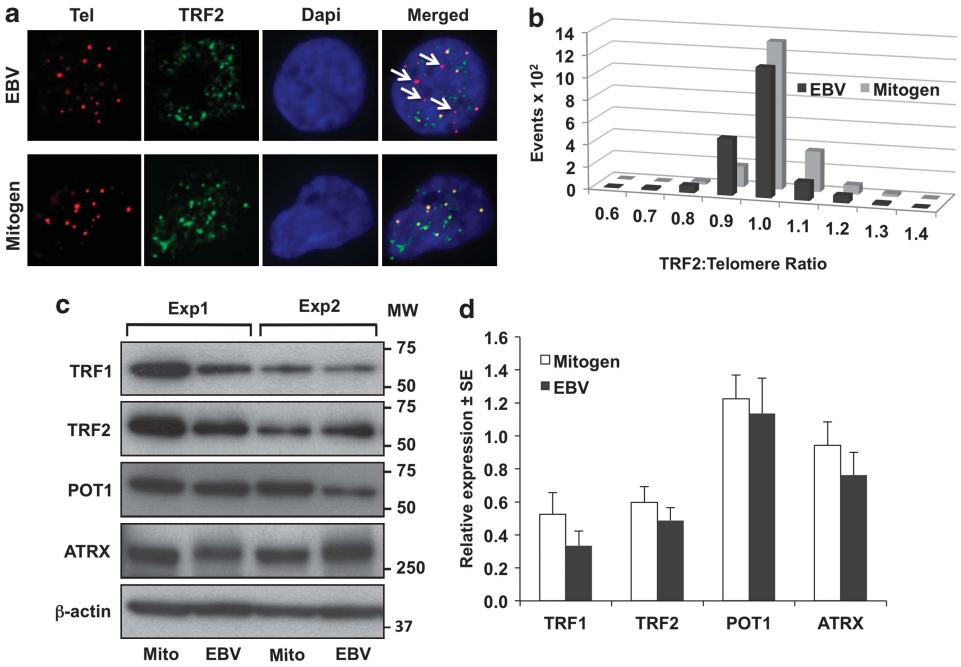

Figure 6. EBV infection promotes telomere uncapping. (**a**) Representative micrographs illustrating the presence of uncapped telomeres 2 weeks after EBV infection as assessed by the presence of telomere lacking colocalized TRF2. (**b**) Quantification of telomere localized TRF2 signals. The cells were stained by immunofluorescence-FISH (IF-FISH) and telomeres (red) and TRF2 (green) were identified. The intensity of green fluorescence overlapping with each red telomere was quantified using the MetaExpress software in approximately 2000 telomere signals. A compilation of the data recorded in three independent experiments is shown in the figure. (**c**) Western blot illustrating the expression of components of the shelterin and ATRX/DAXX complexes in EBV-infected or mitogen-induced blasts cultured for 14 days. Total cell lysates were fractioned by sodium dodecyl sulfate–polyacrylamide gel electrophoresis, and blots were probed with the indicated antibodies. (**d**) Densitometry quantification of protein expression. The relative intensity compared with the β-actin-specific band is shown. Mean ± s.e. of five experiments.

the occurrence of double-strand breaks of telomeric sequences;[26,46] (ii) the accumulation of APBs containing PML and telomeric DNA, which serve as scaffolds for the assembly of protein complexes involved in the repair of damaged telomeres by HR[42] and (iii) the high frequency of sister chromatic exchange, confirming the activation of HR-based mechanisms for telomere elongation. This, together with the finding that newly established LCLs have very low or undetectable telomerase activity, suggest that ALT may be the preferred, and in some cases the only mechanism for maintenance of telomere homeostasis during the early phases of EBV-induced B-cell immortalization. It is noteworthy that the low telomerase activity detected in some young LCLs does not diminish the functional significance of ALT in these cells. Indeed, the two mechanism of telomere elongation were shown to coexist in some tumor and established cell lines.[47]

We have found that all signs of ALT are greatly reduced in LCLs kept in culture for extended periods of time in parallel with the activation of telomerase. This finding is in line with the known inhibitory effect of telomerase on recombination-based mechanisms for telomere elongation,[48] and confirms the observation that the activation of telomerase is a late event in EBV-induced B-cell immortalization.[49] It has been suggested that the late activation of telomerase is preceded by a dramatic drop of LCL cell viability, aching to the growth crisis that precedes the establishment of immortal fibroblast cell lines. We have not observed clear signs of growth crisis in LCLs that were kept in continuous culture for >12 months, with the possible exception of occasional transient declines in cell viability that could be due to improper handling of the cultures. Thus, the lack of telomerase activity in young LCLs does not imply that these cells have not achieved 'true immortality'. Indeed, it seems quite possible that the late activation of telomerase may be an artifact of the *in vitro* culture conditions because the high genomic instability associated with ALT[50] entails a growth disadvantage that may favor the outgrowth of telomerase-positive cells. In this context, it should be noted that very little functional data is available on the activity of telomerase in EBV-positive tumors. Particularly informative would be the comparison of telomerase activity in post-transplant lymphoma that arise early or late after transplantation because these tumors are likely to have been exposed to different selective pressure *in vivo*.

Although the details of the process remain largely unknown, recent findings have shed some light on the mechanisms that lead to the activation of ALT (reviewed in Cesare and Reddel[51]). Key events appear to be the loss of factors that normally repress HR at telomeres, such as the shelterin proteins TRF2 and POT1,[24,52] and the chromatin-remodeling complex ATRX/DAXX. The proteins encoded by *ATRX* and *DAXX* have key functions in the remodeling of telomeric heterochromatin and incorporation of the histone variant H3.3.[53] Impaired function of ATRX is associated with increased transcription of TTAGGG telomeric repeats, TERRA, reduced telomeric loading of HP1α, defects in sister chromatid cohesion and aberrant mitoses with formation of micronuclei and chromatin bridges.[54,55] We have found that a significant proportion of telomeres in EBV-infected cell have little or no associated TRF2 within the first 2 weeks of culture in spite of unchanged levels of TRF2 detected in western blot (Figure 6). Conceivably, a change in the ratio of telomeric DNA to the total cellular content of shelterin proteins could result in a relative deficiency of the latter, which may hamper the repression of telomeric recombination. The failure to upregulate TRF1, TRF2, POT1 and ATRX in newly infected cells, together with the low expression of these proteins in newly established LCLs compared with old LCLs (Figure 7), suggests that EBV lacks the capacity to directly regulate their expression and supports the possibility that insufficient amounts of the shelterin and ATRX/DAXX complexes

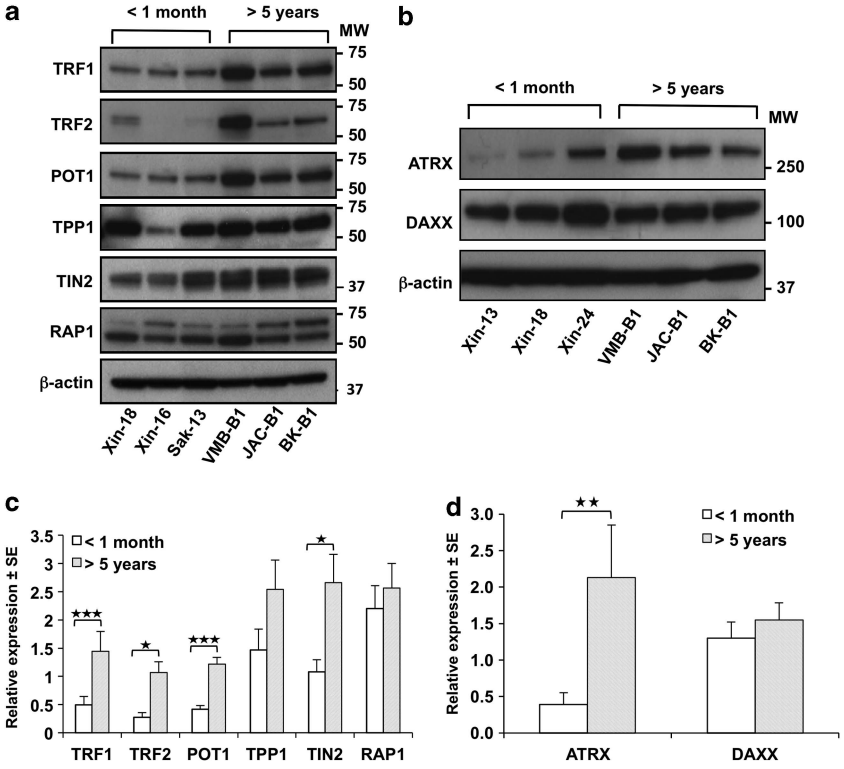

Figure 7. Expression of shelterin proteins and components of the ATRX/DAXX chromatin-remodeling complex in freshly established and old LCLs. (**a**) Representative western blot illustrating the lower expression of components of the shelterin complex in newly established LCLs. (**b**) Representative western blot illustrating the lower expression of the ATRX/DAXX complex in newly established LCLs. (**c**) Quantification of protein expression. Six newly established and six old LCLs were tested in at least three independent experiments. The relative intensity compared with the β-actin-specific band is shown. $^{*}P<0.05$; $^{***}P<0.001$. (**d**) Quantification of protein expression. Six freshly established and six old LCLs were tested in atleast three independent experiments. The relative intensity compared with the β-actin-specific band is shown. $^{**}P<0.01$.

may have a key role in the activation of ALT during the early phases of immortalization. It remains unclear, however, whether the decrease in shelterin protein saturation at telomeres is the cause or the consequence of ALT activation. It is noteworthy that newly infected cells and young LCLs exhibited both longer telomeres (Figures 3 and 4) and extra-chromosomal telomeres (Figures 1 and 2), which together could amount to a significant increase in telomeric DNA. It is also possible that functional inactivation of the shelterin and ATRX/DAXX complexes may occur at the very early stages of infection. An interesting possibility is suggested by our earlier finding that the EBV nuclear antigen EBNA1 promotes genomic instability and telomere dysfunction by transcriptional activation of the catalytic subunit of the NADPH oxidase, NOX2, which correlates with increased oxidative stress and induction of DNA damage.[56] The telomeric G-triplet is particularly sensitive to oxidative stress-mediated damage, which increases the frequency of S1 nuclease-sensitive sites at telomeres and could promote the activation of recombination-based repair (reviewed in von Zglinicki[57]). The oxidative environment may also directly affect the function of the shelterin complex because oxidation disrupts the recognition of telomeric DNA by TRF1 and TRF2.[58]

In conclusion, our findings suggest that ALT has a key role in the rescue of EBV-infected cells from replicative senescence during the early phases of immortalization. The inherently imprecise recombination mechanisms that characterize ALT may also give rise to inappropriate repair and chromosomal aberrations. This scenario is in line with the high frequency of non-clonal chromosomal aberrations in EBNA1 expressing B-lymphoma lines[59] and is also supported by the findings of Lacoste *et al.*[38] that documented high karyotypic instability during the first weeks after EBV infection, followed by the establishment of oligoclonal or monoclonal cell lines. Thus, EBV infection appears to induce several key phenotypic properties of malignant transformation, including autonomous growth, genomic instability and the escape from replicative senescence through activation of recombination-based mechanisms for telomere homeostasis.

MATERIALS AND METHODS

B-cell isolation, EBV infection and mitogen stimulation

Blood lymphocytes were purified from Buffy coats (Blood Bank, Karolinska Hospital, Stockholm, Sweden) by Ficoll–Paque (Lymphoprep, Axis-shield PoC AS, Oslo, Norway) density gradient centrifugation and B cells were affinity purified using CD19 micro beads (MACS MicroBeads, Miltenyi Biotec, Bergisch Gladbach, Germany) according to standard procedures. For EBV infection, the cells were pre-incubated for 1 h with spent supernatant from the EBV producer cell line B95.8,[60] and then cultured in RPMI-1640, supplemented with 10–20% fetal bovine serum, 2 mM L-glutamine, 100 U/ml penicillin and 0.1 mg/ml streptomycin, (all from Sigma-Aldrich, St Louis, MO, USA). EBV gene expression was confirmed by immunofluorescence using specific polyclonal and monoclonal antibodies to the nuclear antigens EBNA1 and EBNA2. For mitogen stimulation, purified B and T cells were incubated with inactivated *S. Aureus* (1/10 000 pansorbin cells, Calbiochem, Merck KGaA, Darmstadt, Germany) or purified phytohemoagglutinine (PHA 5 μg/ml, Sigma-Aldrich), respectively, and expanded in medium containing 20 U/ml recombinant IL-2 (Peprotech, Rocky Hill, NJ, USA). The LCLs: BK-B1, JAC-B1, VMB-B1, IARC-171, WW1-LCL and WW2-LCL obtained by B95.8-induced immortalization of B cells from healthy donors and Burkitt's lymphoma patients were previously described.[61,62] All cells were kept at 37 °C in a humidified atmosphere containing 5% CO_2 and fed twice a week. Cell division was assessed by vital labeling with carboxyfluorescein diacetate succinimidyl ester (C34554, Molecular Probes, Life Technologies Europe, Stockholm, Sweden)[63] and DNA content was examined by propidium iodide staining.

Immunoblotting

Cell lysates were prepared in lithium dodecyl sulfate sample buffer, fractionated in precast 4–12% sodium dodecyl sulfate–polyacrylamide gel electrophoresis gradient gels (Invitrogen Corp., Carlsbad, CA, USA) and transferred to polyvinylidene fluoride membranes (Millipore Corporation, Bedford, MA, USA). The blots were probed with antibodies to TRF1 (1:1000 sc.56807, Santa Cruz, CA, USA), TRF2 (1:1000, IMG124A, IMGENEX, San Diego, CA, USA), POT1 (1:1000 NB500-176, Novus Biologicals, Littleton, CO, USA), TPP1 (1:500 ab39042, Abcam, Cambridge, MA, USA), TIN2 (1:250 IMG-282, IMGENEX), RAP-1 (1:1000 NB100-292, Novus Biologicals), ATRX (1:1000 H-300, Sc-15408, Santa Cruz), DAXX (1:1000 D7810, Sigma-Aldrich) and β-actin (1:20 000 A5441, Sigma-Aldrich) followed by the appropriate horseradish peroxidase-conjugated secondary antibody (Zymed, San Francisco, CA, USA), developed by enhanced chemiluminescence (GE Healthcare Limited, Buckinghamshire, UK) and analyzed using the Fuji LAS 1000 system (FujiFilm Medical Systems Inc., Stamford, CT, USA).

Quantitative fluorescence *in situ* hybridization

The cells were treated with 30 ng/ml colcemide (KaryoMAX, Invitrogen Corp.) for 90 min to induce metaphase arrest, washed in hypotonic buffer containing 75 mM KCl (Sigma-Aldrich), fixed in methanol acetic acid (3:1) and dropped onto cold glass slides. The slides were fixed in 4% formaldehyde (Merck) for 5 min, treated with 1 mg/ml pepsin for 10 min at 37 °C and dehydrated by consecutive 5-min incubations in 70%, 85% and 100% cold ethanol. After air drying, hybridization solution containing the Telomere PNA probe (Panagene, Cambridge Research Biomedicals, Cleveland, UK) was added, followed by heat denaturation for 3 min at 80 °C. Hybridization was allowed to proceed for 2 h at room temperature in the dark. The slides were then overlaid with washing solutions, dehydrated and mounted with 4,6-diamidino-2-phenylindole-containing Vectashield (Vector Laboratories, Inc. Burlingame, CA, USA). Digital images were captured with a LEITZ LEITZBMRB fluorescence microscope (Leica, Wetzlar, Germany) equipped with a CCD camera (Hamamatsu Photonic Norden AB, Kista, Sweden). The presence of telomere abnormalities, including telomere fusions and extra chromosomal telomere, were scored in digital images using Adobe Photoshop (Adobe Systems Inc., San Jose, CA, USA). The fluorescence intensity of each telomere signal was scored using the Volocity Software (Improvision, University of Warwick Science Park, UK). The results are expressed as fluorescence intensity of telomeres in 25 randomly selected metaphase plates from three independent experiments.

Detection of APBs and telomere-associated TRF2 by immunofluorescence-FISH

Three $\times 10^4$ cells in 0.1 ml phosphate-buffered saline were deposited on glass slides by cytospin centrifugation, fixed in freshly prepared 3.7% formaldehyde for 10 min and permeabilized with 0.1% Triton X-100 (T9284, Sigma-Aldrich) for 5 min. After blocking with 3% fetal calf serum for 30 min, the slides were incubated for 1 h at room temperature with a mouse monoclonal antibody to PML (1:100, kind gift of Hugues de Thé, University of Paris, Paris, France), or overnight at 4 °C with rabbit polyclonal antibody to TRF2 (1:100, Sc-9143, Santa Cruz), followed by Alexa Fluor 488-conjugated donkey anti-mouse or anti-rabbit antibodies (Invitrogen Corp.) for 30 min. After washing and fixation with 3.7% formaldehyde for 5 min and dehydration in increasing concentrations of ethanol, Q-FISH was performed as described above. The presence of APBs was scored in digital images captured using a LSM 510 Meta microscope (Carl Zeiss, Carl Zeiss AB, Stockholm, Sweden) based on colocalization of PML and telomere signals on a single focal plane using the ImagJ software (http://rsb.info.nih.gov). For quantification of telomere-associated TRF2, digital images were captured with an ImageXpress Micro device (Molecular Devices, Sunnyvale, CA, USA) and analyzed with the MetaExpress Software (Molecular Devices). Two thousand telomere signals were identified in multiple images from each experimental condition and the intensity of red (telomere) and green (TRF2) fluorescence within each selected telomere area was quantified.

Detection of telomere sister chromatid exchanges by chromosome orientation-FISH

The cells were grown in medium containing 10 μM BrdU (Sigma-Aldrich) and BrdC (MP Biomedicals, Illkirch, France) at 3:1 ratio for 16 h and chromosome slides were prepared as described. After treatment with 0.5 mg/ml RNAase A (Invitrogen Corp.) for 10 min at 37 °C, staining with 0.5 μg/ml Hoechst 33258 in 2 × SSC for 15 min at room temperature and cross-linking by exposure to 365-nm UV light (Stratalinker 1800, Agilent Technologies, St Clara, CA, USA) for 30 min, the slides were digested with 10 U/μl Exonuclease III (Fermentas, Leon-Rot, Germany) for 10 min at room temperature and sequentially incubated with TAMRA-TelG 5′-(TTAGGG)3-3′ and FITC-TelC 5′-[CCCTAA]3-3′ probes (Cambridge Research Biomedicals) at room temperature for 2 h followed by washing, dehydration and mounting with 4,6-diamidino-2-phenylindole-containing Vectashield. Digital images were analyzed as described.

Detection of telomerase activity by TRAP

Telomerase activity was measured using the TRAPeze telomerase detection kit (S7700, Millipore Corporation, Billerica, MA, USA). Briefly, 10^6 cells were lysed in 200 μl of 3-[(3-cholamidopropyl)dimethylammonio]-1-propanesulfonate (CHAPS) lysis buffer supplemented with 200 U/ml of RNAse inhibitor (N211B, Promega, Madison WI, USA). After clearing by centrifugation at 14 000 *g* for 20 min at 4 °C, the protein concentration of the supernatant was measured using the Bio-Rad protein assay kit (Bio-Rad Laboratories AB, Solna, Sweden). The reactions were carried out with 0.1 μg of cell lysate in 25 μl of TRAP buffer, containing dNTP, primers and DNA polymerase (F120S, Hot Start DNA Polymerase, BioLabs, Inc., Ipswich, UK). Cell lysates provided by the kit were used as positive control and lysates of the telomerase negative U2OS cell line were used to determine the background activity of the assays. Telomere extension was performed at 30 °C for 30 min, followed by 28 PCR cycles including denaturation at 94 °C for 5 s, annealing at 61 °C for 30 s and elongation for 1 min at 72 °C. As negative control, the lysates were heated at 85 °C for 10 min to inactivate the telomerase. The PCR products were loaded onto a 10% polyacrylamide denaturing gel and electrophoresis was carried out at 300 V for 2 h, followed by staining with SYBR Gold (S11494, Invitrogen, Eugene, OR, USA), and visualization using a Typhoon 9400 Variable Mode Imager (Amersham Biosciences Corp., Piscataway, NJ, USA). Digital images were analyzed using the Gene Imager software (Amersham Biosciences Corp.) and total product generated units were calculated as indicated by the kit.

Statistical analysis

Statistical analysis was performed using Student's *t*-test. *P*-values <0.05 were considered as significant.

CONFLICT OF INTEREST

The authors declare no conflict of interest.

ACKNOWLEDGEMENTS

This study was supported by grants awarded by the Swedish Cancer Society, the Swedish Medical Research Council and the Karolinska Institutet, Stockholm, Sweden. XC was supported by a fellowship awarded by the China Scholarship Council.

REFERENCES

1 Blackburn EH. Structure and function of telomeres. *Nature* 1991; **350**: 569–573.
2 de Lange T, Shiue L, Myers RM, Cox DR, Naylor SL, Killery AM *et al.* Structure and variability of human chromosome ends. *Mol Cell Biol* 1990; **10**: 518–527.
3 Griffith JD, Comeau L, Rosenfield S, Stansel RM, Bianchi A, Moss H *et al.* Mammalian telomeres end in a large duplex loop. *Cell* 1999; **97**: 503–514.
4 Makarov VL, Hirose Y, Langmore JP. Long G tails at both ends of human chromosomes suggest a C strand degradation mechanism for telomere shortening. *Cell* 1997; **88**: 657–666.
5 de Lange T. Shelterin: the protein complex that shapes and safeguards human telomeres. *Genes Dev* 2005; **19**: 2100–2110.
6 Palm W, de Lange T. How shelterin protects mammalian telomeres. *Annu Rev Genet* 2008; **42**: 301–334.
7 O'Connor MS, Safari A, Xin H, Liu D, Songyang Z. A critical role for TPP1 and TIN2 interaction in high-order telomeric complex assembly. *Proc Natl Acad Sci USA* 2006; **103**: 11874–11879.
8 Walker JR, Zhu XD. Post-translational modifications of TRF1 and TRF2 and their roles in telomere maintenance. *Mech Ageing Dev* 2012; **133**: 421–434.
9 van Steensel B, de Lange T. Control of telomere length by the human telomeric protein TRF1. *Nature* 1997; **385**: 740–743.
10 Denchi EL, de Lange T. Protection of telomeres through independent control of ATM and ATR by TRF2 and POT1. *Nature* 2007; **448**: 1068–1071.
11 van Steensel B, Smogorzewska A, de Lange T. TRF2 protects human telomeres from end-to-end fusions. *Cell* 1998; **92**: 401–413.

12 Karlseder J, Broccoli D, Dai Y, Hardy S, de Lange T. p53- and ATM-dependent apoptosis induced by telomeres lacking TRF2. *Science* 1999; **283**: 1321–1325.
13 Hockemeyer D, Sfeir AJ, Shay JW, Wright WE, de Lange T. POT1 protects telomeres from a transient DNA damage response and determines how human chromosomes end. *EMBO J* 2005; **24**: 2667–2678.
14 Kim SH, Beausejour C, Davalos AR, Kaminker P, Heo SJ, Campisi J. TIN2 mediates functions of TRF2 at human telomeres. *J Biol Chem* 2004; **279**: 43799–43804.
15 Shay JW, Pereira-Smith OM, Wright WE. A role for both RB and p53 in the regulation of human cellular senescence. *Exp Cell Res* 1991; **196**: 33–39.
16 Takai H, Smogorzewska A, de Lange T. DNA damage foci at dysfunctional telomeres. *Curr Biol* 2003; **13**: 1549–1556.
17 Karlseder J, Smogorzewska A, de Lange T. Senescence induced by altered telomere state, not telomere loss. *Science* 2002; **295**: 2446–2449.
18 Shay JW, Bacchetti S. A survey of telomerase activity in human cancer. *Eur J Cancer* 1997; **33**: 787–791.
19 Bryan TM, Englezou A, Gupta J, Bacchetti S, Reddel RR. Telomere elongation in immortal human cells without detectable telomerase activity. *EMBO J* 1995; **14**: 4240–4248.
20 Bryan TM, Englezou A, Dalla-Pozza L, Dunham MA, Reddel RR. Evidence for an alternative mechanism for maintaining telomere length in human tumors and tumor-derived cell lines. *Nat Med* 1997; **3**: 1271–1274.
21 Dunham MA, Neumann AA, Fasching CL, Reddel RR. Telomere maintenance by recombination in human cells. *Nat Genet* 2000; **26**: 447–450.
22 Yeager TR, Neumann AA, Englezou A, Huschtscha LI, Noble JR, Reddel RR. Telomerase-negative immortalized human cells contain a novel type of promyelocytic leukemia (PML) body. *Cancer Res* 1999; **59**: 4175–4179.
23 Bechter OE, Zou Y, Shay JW, Wright WE. Homologous recombination in human telomerase-positive and ALT cells occurs with the same frequency. *EMBO Rep* 2003; **4**: 1138–1143.
24 Celli GB, Denchi EL, de Lange T. Ku70 stimulates fusion of dysfunctional telomeres yet protects chromosome ends from homologous recombination. *Nat Cell Biol* 2006; **8**: 885–890.
25 Sfeir A, Kabir S, van Overbeek M, Celli GB, de Lange T. Loss of Rap1 induces telomere recombination in the absence of NHEJ or a DNA damage signal. *Science* 2010; **327**: 1657–1661.
26 Wang RC, Smogorzewska A, de Lange T. Homologous recombination generates T-loop-sized deletions at human telomeres. *Cell* 2004; **119**: 355–368.
27 Lovejoy CA, Li W, Reisenweber S, Thongthip S, Bruno J, de Lange T *et al.* Loss of ATRX, genome instability, and an altered DNA damage response are hallmarks of the alternative lengthening of telomeres pathway. *PLoS Genet* 2012; **8**: e1002772.
28 Young LS, Rickinson AB. Epstein-Barr virus: 40 years on. *Nat Rev Cancer* 2004; **4**: 757–768.
29 Xia T, O'Hara A, Araujo I, Barreto J, Carvalho E, Sapucaia JB *et al.* EBV microRNAs in primary lymphomas and targeting of CXCL-11 by ebv-mir-BHRF1-3. *Cancer Res* 2008; **68**: 1436–1442.
30 Young LS, Murray PG. Epstein-Barr virus and oncogenesis: from latent genes to tumours. *Oncogene* 2003; **22**: 5108–5121.
31 Purtilo DT, Strobach RS, Okano M, Davis JR. Epstein-Barr virus-associated lymphoproliferative disorders. *Lab Invest* 1992; **67**: 5–23.
32 Bird AG, McLachlan SM, Britton S. Cyclosporin A promotes spontaneous outgrowth *in vitro* of Epstein-Barr virus-induced B-cell lines. *Nature* 1981; **289**: 300–301.
33 Mei YP, Zhu XF, Zhou JM, Huang H, Deng R, Zeng YX. siRNA targeting LMP1-induced apoptosis in EBV-positive lymphoma cells is associated with inhibition of telomerase activity and expression. *Cancer Lett* 2006; **232**: 189–198.
34 Terrin L, Dal Col J, Rampazzo E, Zancai P, Pedrotti M, Ammirabile G *et al.* Latent membrane protein 1 of Epstein-Barr virus activates the hTERT promoter and enhances telomerase activity in B lymphocytes. *J Virol* 2008; **82**: 10175–10187.
35 Yang J, Deng X, Deng L, Gu H, Fan W, Cao Y. Telomerase activation by Epstein-Barr virus latent membrane protein 1 is associated with c-Myc expression in human nasopharyngeal epithelial cells. *J Exp Clin Cancer Res* 2004; **23**: 495–506.
36 Chen F, Liu C, Lindvall C, Xu D, Ernberg I. Epstein-Barr virus latent membrane 2A (LMP2A) down-regulates telomerase reverse transcriptase (hTERT) in epithelial cell lines. *Int J Cancer* 2005; **113**: 284–289.
37 Sugimoto M, Tahara H, Ide T, Furuichi Y. Steps involved in immortalization and tumorigenesis in human B-lymphoblastoid cell lines transformed by Epstein-Barr virus. *Cancer Res* 2004; **64**: 3361–3364.
38 Lacoste S, Wiechec E, Dos Santos Silva AG, Guffei A, Williams G, Lowbeer M *et al.* Chromosomal rearrangements after ex vivo Epstein-Barr virus (EBV) infection of human B cells. *Oncogene* 2010; **29**: 503–515.
39 Sugimoto M, Ide T, Goto M, Furuichi Y. Reconsideration of senescence, immortalization and telomere maintenance of Epstein-Barr virus-transformed human B-lymphoblastoid cell lines. *Mech Ageing Dev* 1999; **107**: 51–60.
40 Ford LP, Zou Y, Pongracz K, Gryaznov SM, Shay JW, Wright WE. Telomerase can inhibit the recombination-based pathway of telomere maintenance in human cells. *J Biol Chem* 2001; **276**: 32198–32203.
41 Henson JD, Reddel RR. Assaying and investigating alternative lengthening of telomeres activity in human cells and cancers. *FEBS Lett* 2010; **584**: 3800–3811.
42 Chung I, Osterwald S, Deeg KI, Rippe K. PML body meets telomere: the beginning of an ALTernate ending? *Nucleus* 2012; **3**: 263–275.
43 Nikitin PA, Yan CM, Forte E, Bocedi A, Tourigny JP, White RE *et al.* An ATM/Chk2-mediated DNA damage-responsive signaling pathway suppresses Epstein-Barr virus transformation of primary human B cells. *Cell Host Microbe* 2010; **8**: 510–522.
44 Martinez P, Blasco MA. Telomeric and extra-telomeric roles for telomerase and the telomere-binding proteins. *Nat Rev Cancer* 2011; **11**: 161–176.
45 Bellon M, Nicot C. Regulation of telomerase and telomeres: human tumor viruses take control. *J Natl Cancer Inst* 2008; **100**: 98–108.
46 Henson JD, Cao Y, Huschtscha LI, Chang AC, Au AY, Pickett HA *et al.* DNA C-circles are specific and quantifiable markers of alternative-lengthening-of-telomeres activity. *Nat Biotechnol* 2009; **27**: 1181–1185.
47 Cerone MA, Londono-Vallejo JA, Bacchetti S. Telomere maintenance by telomerase and by recombination can coexist in human cells. *Hum Mol Gen* 2001; **10**: 1945–1952.
48 Hu J, Hwang SS, Liesa M, Gan B, Sahin E, Jaskelioff M *et al.* Antitelomerase therapy provokes ALT and mitochondrial adaptive mechanisms in cancer. *Cell* 2012; **148**: 651–663.
49 Kataoka H, Tahara H, Watanabe T, Sugawara M, Ide T, Goto M *et al.* Immortalization of immunologically committed Epstein-Barr virus-transformed human B-lymphoblastoid cell lines accompanied by a strong telomerase activity. *Differentiation* 1997; **62**: 203–211.
50 Royle NJ, Foxon J, Jeyapalan JN, Mendez-Bermudez A, Novo CL, Williams J *et al.* Telomere length maintenance--an ALTernative mechanism. *Cytogen Gen Res* 2008; **122**: 281–291.
51 Cesare AJ, Reddel RR. Alternative lengthening of telomeres: models, mechanisms and implications. *Nat Rev Genet* 2010; **11**: 319–330.
52 He H, Multani AS, Cosme-Blanco W, Tahara H, Ma J, Pathak S *et al.* POT1b protects telomeres from end-to-end chromosomal fusions and aberrant homologous recombination. *EMBO J* 2006; **25**: 5180–5190.
53 De La Fuente R, Baumann C, Viveiros MM. Role of ATRX in chromatin structure and function: implications for chromosome instability and human disease. *Reproduction* 2011; **142**: 221–234.
54 Azzalin CM, Reichenbach P, Khoriauli L, Giulotto E, Lingner J. Telomeric repeat containing RNA and RNA surveillance factors at mammalian chromosome ends. *Science* 2007; **318**: 798–801.
55 Ritchie K, Seah C, Moulin J, Isaac C, Dick F, Berube NG. Loss of ATRX leads to chromosome cohesion and congression defects. *J Cell Biol* 2008; **180**: 315–324.
56 Gruhne B, Sompallae R, Marescotti D, Kamranvar SA, Gastaldello S, Masucci MG. The Epstein-Barr virus nuclear antigen-1 promotes genomic instability via induction of reactive oxygen species. *Proc Natl Acad Sci USA* 2009; **106**: 2313–2318.
57 von Zglinicki T. Role of oxidative stress in telomere length regulation and replicative senescence. *Ann N Y Acad Sci* 2000; **908**: 99–110.
58 Opresko PL, Fan J, Danzy S, Wilson 3rd DM, Bohr VA. Oxidative damage in telomeric DNA disrupts recognition by TRF1 and TRF2. *Nucleic Acids Res* 2005; **33**: 1230–1239.
59 Kamranvar SA, Gruhne B, Szeles A, Masucci MG. Epstein-Barr virus promotes genomic instability in Burkitt's lymphoma. *Oncogene* 2007; **26**: 5115–5123.
60 Miller G, Shope T, Lisco H, Stitt D, Lipman M. Epstein-Barr virus: transformation, cytopathic changes, and viral antigens in squirrel monkey and marmoset leukocytes. *Proc Natl Acad Sci USA* 1972; **69**: 383–387.
61 Lenoir GM, Vuillaume M, Bonnardel C. The use of lymphomatous and lymphoblastoid cell lines in the study of Burkitt's lymphoma. *IARC Sci Publ* 1985; **60**: 308–318.
62 Torsteinsdottir S, Cuomo L, Klein E, Masucci MG. Stimulation with allogeneic Epstein-Barr virus-transformed lymphoblastoid cell lines generates HLA class I-specific CTLs with different target cell avidity. *Cell Immunol* 1991; **137**: 501–513.
63 Parish CR, Glidden MH, Quah BJ, Warren HS. Use of the intracellular fluorescent dye CFSE to monitor lymphocyte migration and proliferation. *Current Prot Immunol* 2009; **84**: 4.9.1–4.9.13.